Affine-Invariant Multi-reference Shape Priors for Active Contours

Alban Foulonneau[1], Pierre Charbonnier[1], and Fabrice Heitz[2]

[1] ERA 27 LCPC, Laboratoire des Ponts et Chaussées 11 rue Jean Mentelin, B.P. 9, 67035 Strasbourg, France
Alban.Foulonneau@equipement.gouv.fr,
Pierre.Charbonnier@equipement.gouv.fr
[2] Laboratoire des Sciences de l'Image, de l'Informatique et de la Télédétection, UMR 7005 CNRS, Strasbourg I University, Bd Sébastien Brandt, 67400 Illkirch, France
heitz@lsiit.u-strasbg.fr

Abstract. We present a new way of constraining the evolution of a region-based active contour with respect to a set of reference shapes. The approach is based on a description of shapes by the Legendre moments computed from their characteristic function. This provides a region-based representation that can handle arbitrary shape topologies. Moreover, exploiting the properties of moments, it is possible to include intrinsic affine invariance in the descriptor, which solves the issue of shape alignment without increasing the number of d.o.f. of the initial problem and allows introducing geometric shape variabilities. Our new *shape prior* is based on a distance between the *descriptors* of the evolving curve and a reference shape. The proposed model naturally extends to the case where multiple reference shapes are simultaneously considered. Minimizing the *shape energy*, leads to a geometric flow that does not rely on any particular representation of the contour and can be implemented with any contour evolution algorithm. We introduce our prior into a two-class segmentation functional, showing its benefits on segmentation results in presence of severe occlusions and clutter. Examples illustrate the ability of the model to deal with large affine deformation and to take into account a set of reference shapes of different topologies.

1 Introduction

Incorporating global shape constraints into deformable models, which traces back to pioneering works such as [1, 2], has recently received an increasing attention in the context of active contours (see e.g. [3], [4], [5], [6], [7] and references therein). The standard approach consists in defining an additional *prior* term, based on a similarity measure between the evolving shape and a *reference* one. A first important issue that must be dealt with is the question of shape *alignment*. Pose transformations (rotation, translation and scaling) are generally taken into account in an explicit fashion, which increases the number of d.o.f. of the problem, and leads to systems of coupled partial differential equations (PDE's). A second

A. Leonardis, H. Bischof, and A. Pinz (Eds.): ECCV 2006, Part II, LNCS 3952, pp. 601–613, 2006.

issue is the question of *variability*. Variations of the shape away from a reference template are, in the majority of existing works, handled using statistical models, even if a framework that accounts for geometric transformations of the reference shape has recently been proposed in [6].

In this paper, we introduce a novel approach for image segmentation, which combines a parametric representation of shapes with curve evolution theory to constrain the geometry of an evolving active contour toward a given reference shape or a set of reference shapes. More specifically, we consider a parametric description based on Legendre moments computed from the characteristic function of a shape. Such a representation is region-based, does not depend on implementation considerations and allows taking into account arbitrary topologies. Based on this shape description, we define a shape prior as a distance between the evolving curve and a reference shape. This framework naturally extends to the multi-reference case, i.e. when multiple reference shapes are simultaneously considered. Moreover, we exploit the fact that moments convey all geometric information about shape to define a *canonical* representation, i.e. a configuration in which two shapes differing by an affine transformation have identical *descriptors*. Our shape prior is thus intrinsically affine-invariant. This naturally avoids the pose estimation problem and allows the model to handle geometrical variabilities. Finally, a unique evolution equation for the active contour is derived using the formalism of shape derivative and classical differentiation rules as proposed in [8] by Aubert *et al.* Thanks to the ability of the model to change topology during evolution, automatic initialization of the active contour is also possible, whatever the topology of the final target shape.

The reminder of the paper is structured as follows. In Sec. 2, we introduce our new multi-reference, affine-invariant moment-based shape prior. The associated evolution equation is given in Sec. 3. In Sec. 4, we illustrate the benefits of the new prior on the segmentation of objects with various topologies, undergoing large affine transformations, in presence of occlusions and clutter.

2 An Affine-Invariant, Multi-reference Shape Prior

2.1 Encoding Shapes with Moments

Denoting by Ω_{in} the inside region of a shape, the *regular* or *geometric* moments of its characteristic function (which is binary) are defined as:

$$M_{p,q} = \iint_{\Omega_{in}} x^p y^q dxdy \tag{1}$$

where $(p, q) \in \mathbb{Z}^2$, and $(p + q)$ is called the order of the moment. Any shape, discretized on a sufficiently fine grid, may be reconstructed from its infinite set of moments. Hence, when computed from the characteristic function, moments naturally provide region-based *shape descriptors*. However, as is well-known [9], a more tractable representation for reconstruction purposes is obtained by using an orthogonal basis, such as Legendre polynomials:

$$\lambda_{p,q} = C_{pq} \iint_{\Omega_{in}} P_p(x) P_q(y) dx dy, \tag{2}$$

for $(x, y) \in [-1, 1]^2$, where $C_{pq} = (2p + 1)(2q + 1)/4$ is a normalizing constant, and for $x \in [-1, 1]$:

$$P_p(x) = \sum_{k=0}^{p} a_{pk} x^k = \frac{1}{2^p p!} \frac{d^p}{dx^p} (x^2 - 1)^p. \tag{3}$$

Note that there is a linear relationship between Legendre moments and regular moments:

$$\lambda_{p,q} = C_{pq} \sum_{u=0}^{p} \sum_{v=0}^{q} a_{pu} a_{qv} M_{u,v}. \tag{4}$$

In practice we limit this representation to a finite order N and we define the shape descriptor as the D-dimensional vector of Legendre moments: $\boldsymbol{\lambda} = \{\lambda_{p,q}, p+q \leq N\}$, where $D = (N + 1)(N + 2)/2$. Note that this compact description can take into account arbitrary shape topologies.

2.2 Shape Prior Based on Legendre Shape Descriptors

Let us first consider the case where the evolving active contour, Γ, is constrained to evolve toward a *single* reference shape. It is natural to define a shape constraint as a distance d in terms of shape descriptors. Equivalently, in a probabilistic framework, we define a shape prior energy as:

$$J_{prior} = -\log\left(\mathcal{P}(\boldsymbol{\lambda})\right), \tag{5}$$

with:

$$\mathcal{P}(\boldsymbol{\lambda}) \propto \exp\left(-d(\boldsymbol{\lambda}(\Omega_{in}), \boldsymbol{\lambda}^{ref})\right), \tag{6}$$

where Ω_{in} is the inside region of Γ, and $\boldsymbol{\lambda}^{ref}$ is the set of moments of the reference object. In the simplest case d is a quadratic distance. Of course, more elaborate expressions can be used to model arbitrarily complex priors. For example, when N_{ref} reference shapes are simultaneously considered, the above model is extended by defining $\mathcal{P}(\boldsymbol{\lambda})$ as a mixture of pdf's. When d is quadratic and all shapes are equiprobable, this leads to a mixture-of-Gaussians:

$$\mathcal{P}(\boldsymbol{\lambda}) = \frac{1}{N_{ref}} \frac{1}{\sigma\sqrt{2\pi}} \sum_{k=1}^{N_{ref}} \exp\left(-\frac{\|\boldsymbol{\lambda}(\Omega_{in}) - \boldsymbol{\lambda}_{(k)}^{ref}\|^2}{2\sigma^2}\right). \tag{7}$$

In this paper, we will consider multiple-reference models involving different *fixed* shapes. Let us notice that eq. (7) is very close to the classical Parzen density estimator, thus the model readily extends to the definition of *statistical shape variabilities*, in the spirit of [10].

2.3 Handling Pose and Geometric Variabilities

Dealing with affine transformations allows to solve the alignment problem since translation, scaling and rotation are included in this group. Moreover, since transformations such as skewing and reflection are also included, this allows the introduction of geometrical variabilities in the model. For this purpose, we define what we call a *canonical* representation. This is, in fact, a change of variables in which two original shapes, differing by a certain transformation, are represented by the same set of moments. Then, using such a representation for both the reference and the evolving shape straightforwardly makes the model invariant w.r.t. the transformation in question. The advantage of this approach is that the change of variable is defined by closed-form expressions involving only geometric moments, i.e. the data at hand during the optimization stage. No additional optimization over pose parameters is necessary.

For example, in the case of scaling and translation, the canonical representation of a shape is obtained by aligning its centroid, $(\overline{x}, \overline{y})$, with the center of the domain and normalizing its area, $|\Omega_{in}|$, to a constant, $1/\beta$. This amounts to using the *normalized central moments* $\eta_{p,q}$ instead of the $M_{p,q}$'s in (4), as proposed in [11].

$$\eta_{p,q} = \iint_{\Omega_{in}} \frac{(x-\overline{x})^p (y-\overline{y})^q}{(\beta|\Omega_{in}|)^{(p+q+2)/2}} dxdy, \tag{8}$$

$$\text{with} \quad \overline{x} = \frac{M_{1,0}}{M_{0,0}},\ \overline{y} = \frac{M_{0,1}}{M_{0,0}} \text{ and } |\Omega_{in}| = M_{0,0}. \tag{9}$$

In the more general case of affine invariance, our approach is inspired by the *image normalization* procedure [12]. Consider the so-called *compaction* algorithm, which consists first in aligning the ellipse-of-inertia of the shape with the axes of the coordinate system, then, in applying a non-isotropic scaling to make this ellipse circular. It can be shown [12] that two shapes differing by an affine transformation yield the same *compact* shape, up to a rotation. Compensating for this rotation, we obtain a *normalized* shape, which is identical for all affinely-related shapes. Hence, *image normalization* naturally provides our *canonical* representation. Image normalization itself amounts to an affine transformation, i.e. a translation followed by a linear transformation which can be decomposed as:

$$\begin{bmatrix} \cos\gamma & \sin\gamma \\ -\sin\gamma & \cos\gamma \end{bmatrix} \cdot \begin{bmatrix} l_1 & 0 \\ 0 & l_2 \end{bmatrix} \cdot \begin{bmatrix} \cos\theta & \sin\theta \\ -\sin\theta & \cos\theta \end{bmatrix} \tag{10}$$

As already mentioned, the parameters of the *canonical* representation are given by closed-form expressions involving geometric moments. Following [9] and [12], we have:

$$\theta = \frac{1}{2}\text{atan2}\left(\frac{2\nu_{1,1}}{\nu_{2,0} - \nu_{0,2}}\right) \tag{11}$$

where atan2 is the usual four-quadrant inverse tangent,

$$l_{1/2} = \frac{(\nu_{2,0} + \nu_{0,2}) \pm \sqrt{(\nu_{2,0} - \nu_{0,2})^2 + 4\nu_{1,1}^2}}{2} \tag{12}$$

where the $\nu_{u,v}$'s are the second-order central moments of the original shape, and

$$\gamma = \tan^{-1}\left(-\frac{M^c_{1,2}+M^c_{3,0}}{M^c_{0,3}+M^c_{2,1}}\right) + (1-\text{sign}(M^c_{0,3}+M^c_{2,1}))\frac{\pi}{2} \tag{13}$$

where the $M^c_{u,v}$'s are the central moments of the *compact* shape. Image *normalization*, however, does not handle reflection. Since reflection only affects the sign of moments for p odd (reflection w.r.t. y axis) or for q odd (reflection w.r.t. x axis), we choose, without loss of generality, to fix the sign of the third-order moments. *Affine-invariant* moments, yielding the desired *canonical* representation, are finally defined in the following equations:

$$\eta^A_{u,v} = \left(\text{sign}\left(\widehat{\eta}^A_{3,0}\right)\right)^u . \left(\text{sign}\left(\widehat{\eta}^A_{0,3}\right)\right)^v . \widehat{\eta}^A_{u,v}. \tag{14}$$

where:

$$\begin{aligned}\widehat{\eta}^A_{u,v} &= \frac{(l_1.l_2)^{\frac{u+v}{4}}}{(\beta|\Omega_{in}|)^{(u+v+2)/2}} \\ &\times \iint_{\Omega_{in}} \left(\frac{((x-\overline{x})\cos\theta+(y-\overline{y})\sin\theta)}{\sqrt{l_1}}\cos\gamma + \frac{((y-\overline{y})\cos\theta-(x-\overline{x})\sin\theta)}{\sqrt{l_2}}\sin\gamma\right)^u \\ &\times \left(\frac{((y-\overline{y})\cos\theta-(x-\overline{x})\sin\theta)}{\sqrt{l_2}}\cos\gamma - \frac{((x-\overline{x})\cos\theta+(y-\overline{y})\sin\theta)}{\sqrt{l_1}}\sin\gamma\right)^v dxdy.\end{aligned} \tag{15}$$

Note that a simpler model, that only handles rigid transformations may readily be obtained by setting $\gamma = 0$ and $l_1 = l_2 = 1$ in (15) [1].

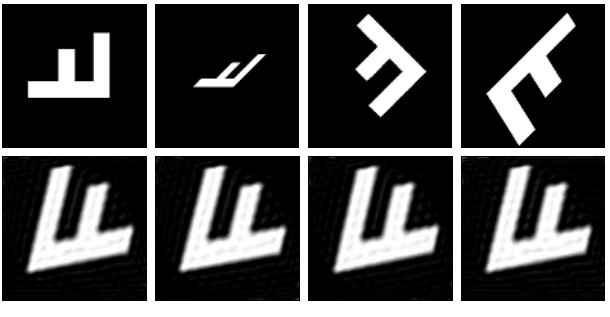

Fig. 1. Reconstruction of shapes from their affine-invariant moments (see text)

Replacing $M_{p,q}$ by $\eta^A_{p,q}$ in (4), we obtain an affine-invariant descriptor that we will denote by $\boldsymbol{\lambda^A}$. Fig. (1) shows examples of reconstruction of four shapes from their affine-invariant descriptor up to the 45th order. The four initial letters

[1] Handling reflection is still necessary in that case, to avoid ambiguity in the determination of θ.

F shown on the upper row are similar up to affine transformations. As it can be seen on the lower row, the four reconstructed shapes are the same. This corresponds to the *canonical* representation and illustrates the invariance of the proposed descriptor.

Using $\boldsymbol{\lambda}^{\boldsymbol{A}}$ instead of $\boldsymbol{\lambda}$ in (5), we define a shape prior which benefits from the affine invariance of the descriptor. This shape constraint, based on the characteristic function, handles complex topologies, does not rely on a particular implementation and is intrinsically invariant w.r.t. affine transformations: the prior has a closed-form expression depending only on moments.

3 Active Contour Evolution Equation

The evolution equation for the boundary of Ω_{in} can be derived from the minimization of J_{prior} using the shape derivative framework [8].

3.1 Single-Reference Model

Let us first focus on the case where the shape constraint is a quadratic distance to as single reference shape, described by $\boldsymbol{\lambda}^{ref}$, i.e.:

$$J_{prior}(\Omega_{in}(t)) = \sum_{p,q}^{p+q\leq N} (\lambda_{p,q}(\Omega_{in}(t)) - \lambda_{p,q}^{ref})^2. \tag{16}$$

When the descriptor is invariant w.r.t. translation and scaling, $\boldsymbol{\lambda}$ and $\boldsymbol{\lambda}^{ref}$ are computed from normalized central moments (8), i.e.:

$$\lambda_{p,q} = C_{pq} \sum_{u=0}^{p} \sum_{v=0}^{q} a_{pu} a_{qv} \eta_{u,v}. \tag{17}$$

Applying the strategy described in [8] in order to minimize J_{prior} leads, in this particular case, to the following flow (see [13] for details):

$$\frac{\partial \Gamma}{\partial t} = \underbrace{\sum_{u,v}^{u+v\leq N} A_{uv} \left(H_{uv}(x,y,\Omega_{int}) + \sum_{i=0}^{2} B_{uvi}.L_i(x,y) \right)}_{V_{prior}} \boldsymbol{\mathcal{N}}, \tag{18}$$

where $\boldsymbol{\mathcal{N}}$ is the inward unit normal vector of Γ and:

$$A_{uv} = 2 \sum_{p,q}^{p+q\leq N} (\lambda_{p,q} - \lambda_{p,q}^{ref}) C_{pq} a_{pu} a_{qv}, \tag{19}$$

$$H_{uv}(x,y,\Omega_{in}) = \frac{(x-\overline{x})^u (y-\overline{y})^v}{|\beta \Omega_{in}|^{(u+v+2)/2}}, \tag{20}$$

$$B_{uv0} = \frac{u.\overline{x}.\eta_{u-1,v} + v.\overline{y}.\eta_{u,v-1}}{\beta^{\frac{1}{2}} |\Omega_{in}|^{\frac{3}{2}}} - \frac{(u+v+2).\eta_{u,v}}{2|\Omega_{in}|}, \tag{21}$$

$$B_{uv1} = \frac{-u.\eta_{u-1,v}}{\beta^{\frac{1}{2}} |\Omega_{in}|^{\frac{3}{2}}}, \quad B_{uv2} = \frac{-v.\eta_{u,v-1}}{\beta^{\frac{1}{2}} |\Omega_{in}|^{\frac{3}{2}}}, \tag{22}$$

$$L_0 = 1, \qquad L_1 = x, \qquad L_2 = y. \tag{23}$$

When taking into account affine invariance in the prior, i.e. using $\boldsymbol{\lambda}^{\boldsymbol{A}}$, we obtain (see [13] for details):

$$\frac{\partial \Gamma}{\partial t} = \underbrace{\sum_{u,v}^{u+v\leq N} A^A_{uv}.\left(\text{sign}\left(\widehat{\eta}^A_{3,0}\right)\right)^u.\left(\text{sign}\left(\widehat{\eta}^A_{0,3}\right)\right)^v.\left(H^A_{uv}+\sum_{i=0}^{9}\widehat{B}^A_{uvi}.L_i\right)}_{V_{prior}}\boldsymbol{\mathcal{N}}, \quad (24)$$

where the expressions of $\widehat{B}^A_{u,v,i}$ are given in [13] and:

$$A^A_{uv} = 2\sum_{p,q}^{p+q\leq N}(\lambda^A_{p,q}-\lambda^{Aref}_{p,q}).C_{pq}a_{pu}a_{qv}, \quad (25)$$

$$H^A_{uv} = \frac{(l_1.l_2)^{\frac{u+v}{4}}}{(|\beta\Omega_{in}|)^{(u+v+2)/2}}$$
$$\times\left(\frac{((x-\overline{x})\cos\theta+(y-\overline{y})\sin\theta}{\sqrt{l_1}}\cos\gamma+\frac{((y-\overline{y})\cos\theta-(x-\overline{x})\sin\theta)}{\sqrt{l_2}}\sin\gamma\right)^u. \quad (26)$$
$$\times\left(\frac{((y-\overline{y})\cos\theta-(x-\overline{x})\sin\theta)}{\sqrt{l_2}}\cos\gamma-\frac{((x-\overline{x})\cos\theta+(y-\overline{y})\sin\theta)}{\sqrt{l_1}}\sin\gamma\right)^v$$

$$L_0 = 1,\ L_1 = x,\ L_2 = y, \quad (27)$$

$$L_3 = x^2,\ L_4 = y^2,\ L_5 = xy, \quad (28)$$

$$L_6 = x^3,\ L_7 = y^3,\ L_8 = x^2y,\ L_9 = xy^2. \quad (29)$$

3.2 Multi-reference Model

Let us now consider the multi-reference case. For the sake of conciseness, we present the case of translation and scale invariance, the case of affine invariance being similar. Taking the log in eq. (7) and differentiating leads to an expression similar to (18), but with a different $A_{u,v}$ factor:

$$\frac{\partial \Gamma}{\partial t} = \underbrace{\sum_{u,v}^{u+v\leq N} A^{multi}_{uv}\left(H_{uv}(x,y,\Omega_{int})+\sum_{i=0}^{2}B_{uvi}.L_i(x,y)\right)}_{V_{prior}}\boldsymbol{\mathcal{N}}, \quad (30)$$

where the expressions of H_{uv}, B_{uvi} and L_i are given by equations (20) to (23). The $A^{multi}_{u,v}$ factor is a weighted average of the individual factors, $A_{(k)uv}$ computed for each reference shape descriptor $\boldsymbol{\lambda}^{ref}_{(k)}$ from (19):

$$A^{multi}_{uv} = \frac{1}{2\sigma^2\sum_{k=1}^{N_{ref}}\exp\left(\frac{-||\boldsymbol{\lambda}-\boldsymbol{\lambda}^{ref}_{(k)}||^2}{2\sigma^2}\right)}\sum_{k=1}^{N_{ref}}A_{(k)uv}\exp\left(\frac{-||\boldsymbol{\lambda}-\boldsymbol{\lambda}^{ref}_{(k)}||^2}{2\sigma^2}\right). \quad (31)$$

In other words, the force induced by the minimization of J_{prior} in the multi-reference case is a weighted average of the individual forces directed towards each reference shape. Note that the weights decay exponentially with the distance in terms of shape descriptors between the evolving curve and the reference shape.

3.3 Implementation

Both the models and the derivation of the active contour evolution equation are independent from any implementation consideration. Consequently, (18) or (24) may be implemented using either a parametric approach, such as spline-snakes [14], or the non-parametric level set formalism [15]. We use here the latter, which naturally handles changes of topology.

4 Application to Image Segmentation

We now address the general problem of two-class segmentation. Our purpose being to illustrate the behavior of the novel prior term, we choose a standard data functional, which was first introduced by Chan and Vese in [16]:

$$J_{data}(\Omega_{in}, \Omega_{out}) = \iint_{\Omega_{in}} (I(x,y) - \mu_{in})^2 dxdy + \iint_{\Omega_{out}} (I(x,y) - \mu_{out})^2 dxdy, \quad (32)$$

where μ_{in} (resp. μ_{out}) is the (unknown) average intensity in the inside (resp. outside) domain, Ω_{in} (resp. Ω_{out}), and $I(x,y)$ is the intensity value of the pixel. Its differentiation may be cast in the general framework presented in [8]. Minimizing the total energy:

$$J(\Omega_{in}, \Omega_{out}) = J_{data}(\Omega_{in}, \Omega_{out}) + \alpha J_{prior}(\Omega_{in}), \quad (33)$$

we obtain:

$$\frac{\partial \Gamma(t)}{\partial t} = (\underbrace{(I - \mu_{in})^2 - (I - \mu_{out})^2}_{V_{data}} + \alpha V_{prior})\boldsymbol{\mathcal{N}}, \quad (34)$$

where V_{prior} is defined in (18), (24) or (30) and μ_{in}, μ_{out} are computed after each iteration [16].

4.1 Single-Reference Model

We illustrate the behavior of our algorithm on the real image of a partially occluded rabbit against a cluttered background (Fig. 3). We first evolve the curve with the region-based energy (32) and an additional standard curvature component. The result (Fig. 3b) is clearly sensitive to the presence of clutter and occlusion. We then refine this result, replacing the curvature term by the shape prior invariant w.r.t. translation and scaling, *i.e.* evolving according to (34) with V_{prior} given by (18). We obtain the final result shown in Fig. 3c. The order of the model, N, is chosen such that the Normalized Mean Squared Error (NMSE) between the reference shape, shown in Fig. 2 (leftmost image), and the reconstruction from its descriptor, given by $\sum_{p=0}^{N} \sum_{q=0}^{p} \lambda_{p-q,q}^{ref} P_{p-q}(x) P_q(y)$, is less than 10%. In the present case, we obtain $N = 40$.

We next consider topologically more complex objects (Fig. 2) against cluttered background and with occlusions (Fig. 4). As in the previous experiment, we first evolve the curve with the region-based energy, then we introduce the shape prior.

Fig. 2. Reference shapes used with the single reference model, eq. (6)

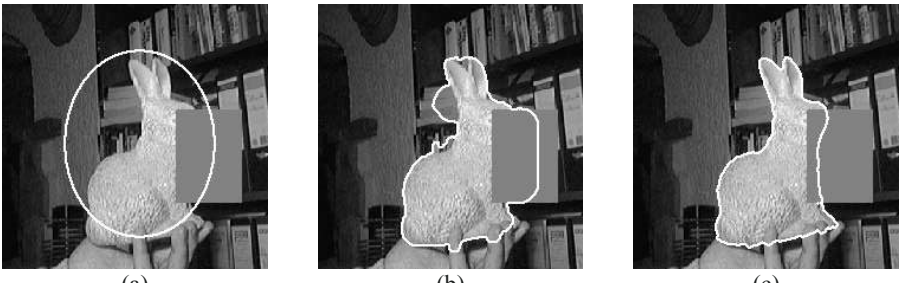

(a) (b) (c)

Fig. 3. Segmentation results on real data (test image: by courtesy of D. Cremers [3]): (a) initial contour, (b) segmentation result without shape prior (standard curvature component used), (c) segmentation result using the single-reference prior (moments up to the 40th-order)

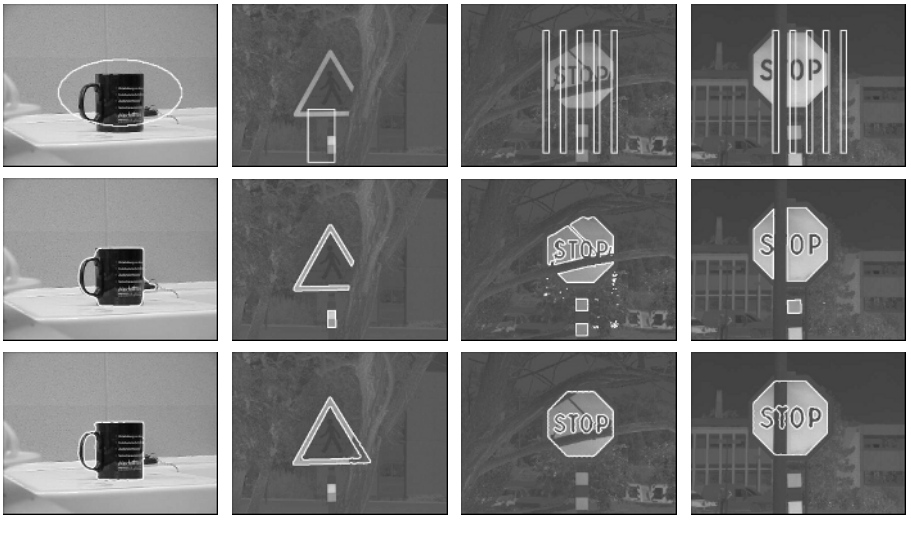

Fig. 4. Segmentation of topologically non-trivial shapes. First row: initial contours (note that they are of different kinds). Second row: results without shape constraint; a curvature term is used for the mug only. Third row: final results, adding the single-reference prior up to the order 40 for the mug and the *stop* sign, up to the order 43 for the *triangle* sign.

The reference shapes are presented on Fig. 2 and the shape prior used in this case is invariant w.r.t. translation and scaling, i.e. V_{prior} is given by (18). Considering for example the third column of Fig. 4, we can see that our prior improves the segmentation result, for a complex shape (the *stop* sign) with important data missing and in presence of noise. Fig. 4 also illustrates the flexibility of our approach w.r.t. the kind of initial curve that is used. Moreover, using the shape constraint, it is possible to overcome the absence of regularization term during the first step of the segmentation.

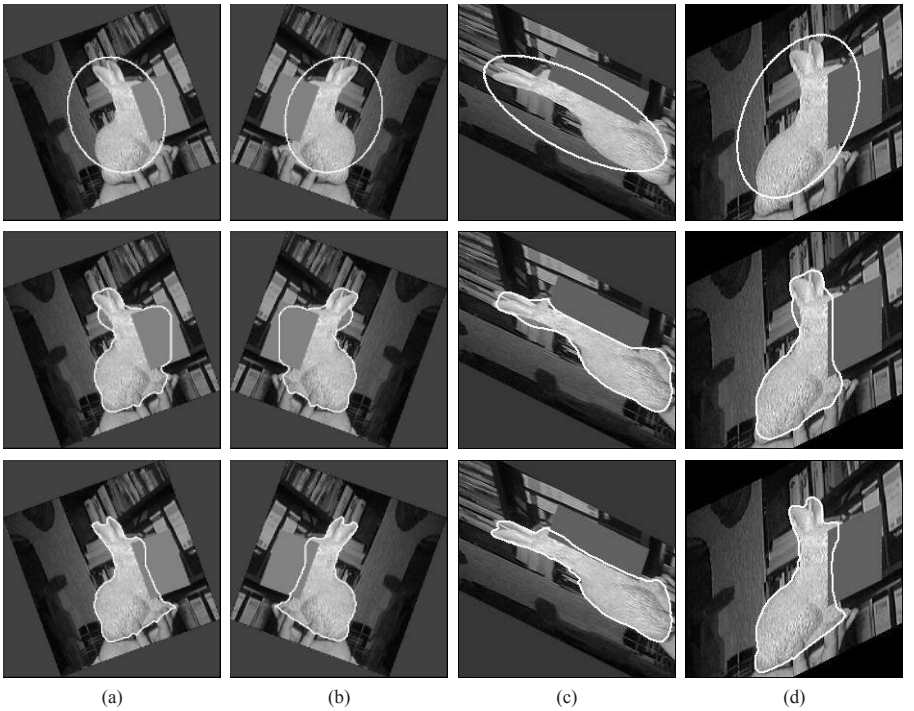

Fig. 5. Segmentation of objects with affine deformations. First row: initial contours. Second row: results without shape constraint (standard curvature component used). Third row: final results, adding the single-reference prior up to the order 40. (a) and (b): the prior is invariant w.r.t. translation, rotation, scaling and reflection. (c) and (d): the full affine model is used.

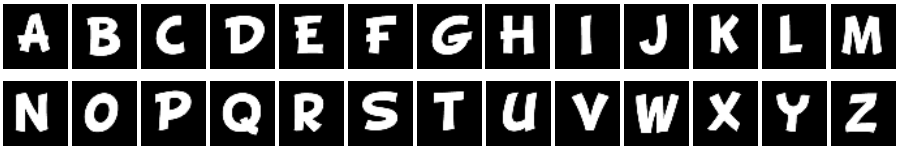

Fig. 6. Set of reference shapes used with the multi-reference model, eq. (7)

Finally, results presented Fig. 5 show the ability of our constraint to deal with large affine deformations of the shape. We use here the flow (24) to regularize the segmentation result. The reference shape is the same as in the experiment presented Fig. 3.

4.2 Multi-reference Model

We now illustrate how the model can take into account several reference shapes in a segmentation application. We consider five images (Fig. 7, first row), each one representing a partially occluded letter. The five segmentation results on the fourth row are obtained with the same curve evolution equation for the contour (34), with V_{prior} given by eq. (30). The constraint is invariant w.r.t. translation and scale. The set of reference shapes, shown Fig. 6, consists of 26 letters. The parameter σ is computed from the set $\{\boldsymbol{\lambda}_{(k)}^{ref}\}$ in order to bound the

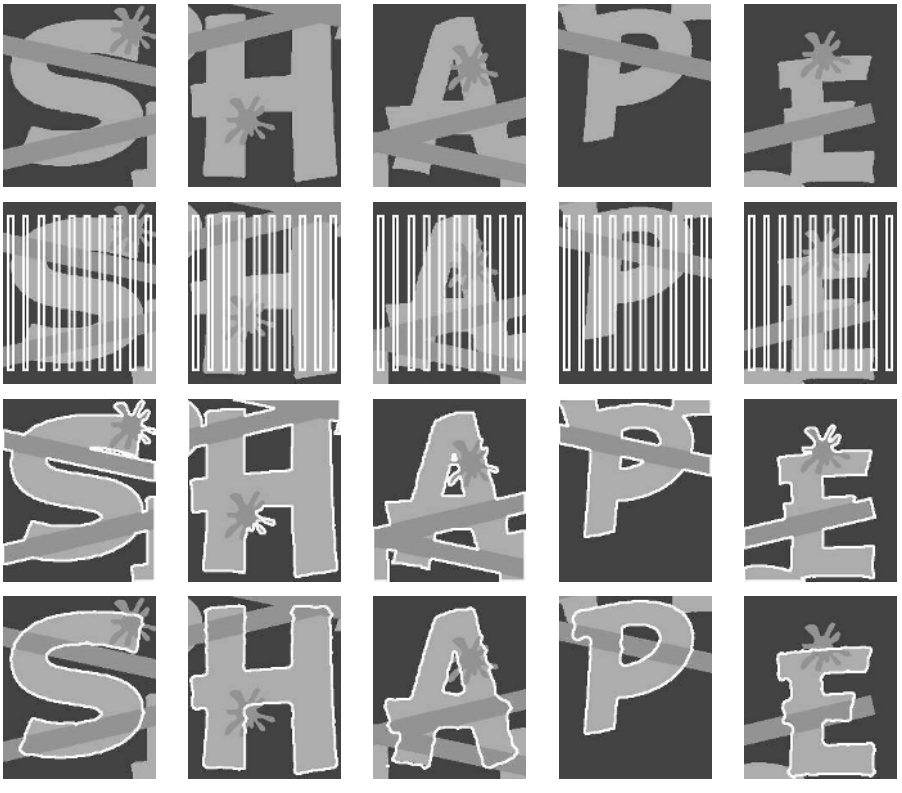

Fig. 7. Segmentation of five images of letters featuring large occlusions. First row: original images. Second row: initialization. Third row: results without shape constraint (no standard curvature component). Fourth row: final results, adding the multi-reference prior up to the order 40. The same set of parameters is used for the whole experiments.

classification error probability, $\mathcal{P}_e$, between the two closest reference shapes in terms of descriptors, where:

$$\mathcal{P}_e = \frac{1}{2} \ \text{erfc}\left(\min_{k \neq l} \frac{\sqrt{||\boldsymbol{\lambda}_{(k)}^{ref} - \boldsymbol{\lambda}_{(l)}^{ref}||^2}}{2\sigma\sqrt{2}} \right) \tag{35}$$

In practice, σ is chosen so that $\mathcal{P}_e < 3\%$.

5 Conclusion

In this paper, we have considered Legendre moments to define affine-invariant shape descriptors. Experimental results show that the obtained evolution equation is able to constrain an active contour to evolve toward a reference shape, and provides robustness to clutter and occlusions in image segmentation. The proposed approach also naturally handles pose variations, affine deformations and complex changes of topology. Moreover, it naturally extends to the multiple-reference case, which paves the way for further extensions to the modeling of statistical shape variabilities.

References

1. Terzopoulos, D., Metaxas, D.: Dynamic 3D models with local and global deformations: Deformable superquadrics. IEEE Transactions on Pattern Analysis and Machine Intelligence **13**(7) (1991) 703–714
2. Cootes, T., Cooper, D., Taylor, C., Graham, J.: Active shape models - their training and application. Computer Vision and Image Understanding **61**(1) (1995) 38–59
3. Cremers, D., Kohlberger, T., Schnörr, C.: Shape statistics in kernel space for variational image segmentation. Pattern Recognition : Special Issue on Kernel and Subspace Methods in Computer Vision **36**(9) (2003) 1929–1943
4. Leventon, M., Grimson, W., Faugeras, O.: Statistical shape influence in geodesic active contours. In: Proc. of IEEE Conference on Computer Vision and Pattern Recognition, Hilton Head Island, Southern Carolina, USA (2000) 1316–1323
5. Rousson, M., Paragios, N.: Shape priors for level set representations. In: Proc. of 7th European Conference on Computer Vision, Lecture Notes in Computer Science. Volume 2351., Copenhaguen, Denmark (2002) 78–93
6. Riklin-Raviv, T., Kiryati, N., Sochen, N.: Unlevel-sets : geometry and prior-based segmentation. In: Proc. of the 8th European Conference on Computer Vision, Lecture Notes in Computer Science. Volume 3024., Prague, Czech (2004) 50–61
7. Tsai, A., Yezzi, A., Wells, W., Tempany, C., Tucker, D., Fan, A., Grimson, W., Willsky, A.: A shape-based approach to the segmentation of medical imagery using level sets. IEEE Transactions on Medical Imaging **22**(2) (2003) 137–154
8. Aubert, G., Barlaud, M., Faugeras, O., Jehan-Besson, S.: Image segmentation using active contours: calculus of variations or shape gradients? SIAM, Journal on Applied Mathematics **63**(6) (2003) 2128–2154
9. Teague, M.: Image analysis via the general theory of moments. Journal of the Optical Society of America **70**(8) (1980) 920–930

10. Cremers, D., Osher, S., Soatto, S.: Kernel density estimation and intrinsic alignment for knowledge-driven segmentation: Teaching level sets to walk. In C. Rasmussen et al., ed.: Pattern Recognition Symposium, Springer, Lecture Notes in Computer Science. Volume 3175., Tübingen, Germany (2004) 36–44
11. Foulonneau, A., Charbonnier, P., Heitz, F.: Geometric shape priors for region-based active contours. In: Proc. of IEEE Conference on Image Processing. Volume 3., Barcelona, Spain (2003) 413–416
12. Pei, S., Lin, C.: Image normalization for pattern recognition. Image and Vision Computing **13**(10) (1995) 711–723
13. Foulonneau, A., Charbonnier, P., Heitz, F.: Affine-invariant geometric shape priors for region-based active contours. Technical Report RR-AF01-2005, LRPC ERA 27 LCPC/LSIIT UMR 7005 CNRS (2005) Available online: http://lsiit-miv.u-strasbg.fr/lsiit/perso/Charbonnier.htm.
14. Precioso, F., Barlaud, M.: B-spline active contour with handling of topology changes for fast video segmentation. Eurasip Journal on Applied Signal Processing, special issue: image analysis for multimedia interactive services - PART II **2002**(6) (2002) 555–560
15. Osher, S., Sethian, J.: Fronts propagating with curvature-dependent speed: algorithms based on Hamilton-Jacobi formulations. Journal of Computational Physics **79**(1) (1988) 12–49
16. Chan, T., Vese, L.: Active contours without edges. IEEE Transactions on Image Processing **10**(2) (2001) 266–277